

# Deletion of CD38 enhances CD19 chimeric antigen receptor T cell function

Kimberly Veliz,<sup>1</sup> Feng Shen,<sup>1</sup> Olga Shestova,<sup>1</sup> Maksim Shestov,<sup>1</sup> Alexander Shestov,<sup>1</sup> Sara Sleiman,<sup>1</sup> Tyler Hansen,<sup>1</sup> Roddy S. O'Connor,<sup>1,2</sup> and Saar Gill<sup>1,3</sup>

<sup>1</sup>Center for Cellular Immunotherapies, University of Pennsylvania, Philadelphia, PA 19104, USA; <sup>2</sup>Parker Institute for Cancer Immunotherapy, University of Pennsylvania, Philadelphia, PA 19104, USA; <sup>3</sup>Cell Therapy and Transplant Program, Division of Hematology-Oncology and Abramson Cancer Center, University of Pennsylvania, Philadelphia, PA 19104, USA

**Cell surface molecules transiently upregulated on activated T cells can play a counter-regulatory role by inhibiting T cell function. Deletion or blockade of such immune checkpoint receptors has been investigated to improve the function of engineered immune effector cells. CD38 is upregulated on activated T cells, and although there have been studies showing that CD38 can play an inhibitory role in T cells, how it does so has not fully been elucidated. In comparison with molecules such as PD1, CTLA4, LAG3, and TIM3, we found that CD38 displays more sustained and intense expression following acute activation. After deleting CD38 from human chimeric antigen receptor (CAR) T cells, we showed relative resistance to exhaustion *in vitro* and improved anti-tumor function *in vivo*. CD38 is a multifunctional ectoenzyme with hydrolase and cyclase activities. Reintroduction of CD38 mutants into T cells lacking CD38 provided further evidence supporting the understanding that CD38 plays a crucial role in producing the immunosuppressive metabolite adenosine and utilizing nicotinamide adenine dinucleotide (NAD) in human T cells. Taken together, these results highlight a role for CD38 as an immunometabolic checkpoint in T cells and lead us to propose CD38 deletion as an additional avenue for boosting CAR T cell function.**

## INTRODUCTION

The stereotyped T cell response to antigen encounter in the setting of appropriate co-stimulation includes proliferation and activation, followed by contraction and memory formation upon pathogen elimination. In the setting of antigen persistence, an exhaustion program is initiated to provide some pathogen control while limiting T cell activation-induced immunopathology.<sup>1,2</sup> Well-characterized inhibitory receptors such as CTLA4, PD1, TIM3, and LAG3 are upregulated early following T cell activation and downregulated upon pathogen clearance; in contrast, their expression is sustained and further increases during T cell exhaustion. These observations have led to clinical trials and regulatory approvals of antibody-based blockade (so-called “immune checkpoint inhibitors” [ICIs]) in patients with cancer.<sup>3</sup> Blockade or elimination of inhibitory immune receptor signaling has also been proposed to improve the function of adoptively transferred immune effector cells such as chimeric antigen receptor T cells (CAR T cells), particularly when antigen persistence

mediates progressive CAR T cell exhaustion.<sup>4–6</sup> Despite multiple pre-clinical studies, clinical reports showing that ICIs compellingly improve CAR T cell function remain scarce.<sup>7–10</sup>

The canonical T cell inhibitory receptors mediate their suppressive functions using their phosphatase or other cytoplasmic domains to inhibit activation pathways downstream of the T cell receptor (PD1, TIM3, and LAG3)<sup>11–13</sup> or by competing for co-stimulatory ligands such as CD80/CD86 (CTLA4).<sup>14</sup> In contrast, the immunometabolic checkpoint molecule CD39, a marker of exhausted tumor-specific CD8 T cells, is an ectoenzyme that breaks down extracellular ATP into AMP, which is then converted to adenosine via CD73. CD39 is therefore thought to inhibit T cells via local production of the immunosuppressive metabolite adenosine, acting through A2A receptors.<sup>15,16</sup>

Additionally, CD39 expression, along with CD38, has been found to be elevated in a subset of T cells that show resistance to anti-PD1 therapy in patients with melanoma.<sup>17</sup> CD38, on the other hand, is a multifunctional ectoenzyme with hydrolase and cyclase activity.<sup>18</sup> CD38 is thought to be the major mammalian nicotinamide adenine dinucleotide (NAD)-consuming enzyme<sup>19</sup> and can also indirectly produce adenosine by hydrolyzing cyclic ADP ribose (cADPR), followed by its conversion to AMP by CD203a and adenosine by CD73. Of these, NAD hydrolysis is thought to be the major enzymatic activity of CD38.<sup>20</sup> NAD<sup>+</sup> is an oxidation reduction substrate for various enzymes including poly(ADP-ribose) polymerases and sirtuins, and in immunocompetent mice, CD38 ablation or blockade improved tumor control that correlated with increased NAD<sup>+</sup> and favorable energetics.<sup>21</sup> CD38 is expressed in dysfunctional tumor-specific murine and human CD8 T cells, including those marked by an exhaustion-specific chromatin state.<sup>22</sup> CD38 serves as a marker for anti-PD1-resistant CD8 T cells in both murine and patient models.<sup>23</sup> In murine models, CD38-mediated adenosine production is implicated in tumor

Received 19 February 2024; accepted 22 May 2024;  
<https://doi.org/10.1016/j.omton.2024.200819>

**Correspondence:** Saar Gill, Center for Cellular Immunotherapies, University of Pennsylvania, Philadelphia, PA 19104, USA.

**E-mail:** [saargill@pennmedicine.upenn.edu](mailto:saargill@pennmedicine.upenn.edu)



escape from PD1 pathway blockade.<sup>24</sup> Moreover, CD38 is postulated to modulate the T cell response through the RyR2 axis, enhancing calcium signaling and reducing the expression of transcription factors like TCF1.<sup>25</sup> Tumor-infiltrating CD4 T cells that express CD38 and CD39 are distinct from regulatory T cells (Tregs) but can also inhibit the proliferation of bystander T cells, suggesting that ectoenzyme activity can function in a cell-extrinsic manner.<sup>26,17</sup>

In human natural killer (NK) cells, deletion of CD38 has been shown to reprogram NK cells toward increased oxidative metabolism and enhanced *in vitro* antibody-dependent cellular cytotoxicity by some groups<sup>27,28</sup> but not others.<sup>29</sup> Recently, CD38-targeting CD38 knockout (CD38KO) CAR T cells have demonstrated enhanced efficacy in controlling T cell acute lymphoblastic leukemia *in vitro* and *in vivo*, particularly against Jurkat cells.<sup>30</sup> Moreover, chemical inhibition of CD38 in CAR T cells has been associated with improved tumor control *in vivo* and increased NAD<sup>+</sup> availability.<sup>31</sup> Our study not only validates these previous findings but also provides further insights into the metabolic consequences of CD38KO in T cells. This underscores the ongoing importance of investigating the role of CD38 in the context of CAR T cells. To better understand the contribution of CD38 to human CAR T cells, we conducted a series of functional experiments both *in vitro* and *in vivo* using anti-CD19 CAR T cells with CRISPR-Cas9 ablation of CD38 expression.

## RESULTS

### CD38 is not required for the short-term function of CAR T cells

To place CD38 in the context of published clinical results, we first reanalyzed publicly available head and neck squamous cell carcinoma (HNSCC) data from 32 donors (6 healthy and 26 HNSCC donors).<sup>32</sup> CD38 clearly clustered with other bona fide T cell activation/exhaustion markers (Figure S1). To establish the kinetics of immune checkpoint molecule expression during the stimulation of human T cells, we added peripheral blood mononuclear cells (PBMCs) to anti-CD3/CD28 beads and followed the expression of PD1, TIM3, LAG3, CTLA4, and CD38 for up to 19 days. In comparison to the activation-associated transient upregulation of PD1, TIM3, LAG3 and CTLA4, we found that CD38 upregulation was more profound and protracted (Figures 1A and 1B). We then set out to determine the impact of eliminating CD38 expression on CAR T cells, using deletion of PD1 (*PDCDI*) as a positive control condition. T cells were transduced with lentiviral supernatant encoding a second-generation 41BB co-stimulated anti-CD19 CAR and expanded as per standard protocol (Figure S2).<sup>33</sup> Deletion of CD38 or PD1 had no effect on CAR T cell proliferation in a short-term *in vitro* assay (Figure 1D), including a direct internal comparison of CD38<sup>-</sup> and residual CD38<sup>+</sup> T cells in the same well (Figures 1C–1E). Additionally, no difference in proliferation was seen, where the percentage of proliferation was measured on day 5 using CellTrace Violet and showed mean cell divisions of 79.4%, 81.9%, and 79.7% for non-transduced (NTC), CD38KO, and PD1KO T cells, respectively (Figure S2D). Given previous reports of metabolic changes, including increased oxidative phosphorylation in CD38-deficient T cells and NK cells, we then measured

the oxygen consumption rate (OCR) as a proxy for oxidative phosphorylation metabolism and the extracellular acidification rate (ECAR) as a proxy for glycolysis consumption. There were no apparent differences in the OCR or ECAR when CD38KO or PD1KO CAR19T cells were compared to controls (Figure 1F). Finally, we performed a 24 h killing assay, incubating a CD19-expressing acute lymphoblastic leukemia cell line with CAR19 T cells at decreasing effector-to-target ratios. Again, there was no difference in the cytolysis of target cells (Figure 1G). Thus, the deletion of CD38 or PD1 has no effect on short-term T cell function *in vitro*.

### Deletion of CD38 mitigates dysfunction in chronically stimulated CAR T cells and improves long-term tumor control

To model T cell exhaustion *in vitro*, we created a model wherein adherent green fluorescence protein (GFP)/Luc<sup>+</sup> AsPC1 cells engineered to express CD19 were incubated with CAR19 T cells; every 3 days, non-adherent cells were removed and added to a new plate of adherent target cells for repeated stimulation (Figure 2A). The quantification of the remaining tumor cells was plotted over time, and better tumor control was seen when cells were incubated with CD38KO and PD1KO CAR19 T cells compared to NTC CAR19 T cells from days 12 to 29 (Figure 2B). Additionally, we saw that at days 9 and 12, there was significantly higher production of interleukin (IL)-2 in CD38KO or PD1KO CAR19 T cells compared to NTC CAR19 T cells (Figure 2C). We saw similar results when using an acute myeloid leukemia tumor model, where CD38KO CAR123 T cells were better at controlling tumor burden than NTC CAR123 T cells (Figure S3). To determine anti-tumor activity *in vivo*, we injected NOD-SCID *IL-2Rγ*<sup>-/-</sup> (NSG) mice with GFP/Luc<sup>+</sup> Nalm6 and treated them with either untransduced (UTD), NTC, CD38KO, or PD1KO CAR19 T cells 7 days after tumor injection (Figure 2D). CD38KO and PD1KO groups exhibit modestly improved tumor control, which translated to improved survival compared to NTC CAR19 T cells (Figures 2E and 2F). These data confirm that CD38KO improves T cell tumor control in a restimulation model and prolongs the survival of mice.

### Metabolic analysis of T cells with CD38KO and mutant expressions

Given the distinctive enzymatic expression of CD38 and prior research highlighting NAD's role in T cell metabolic reprogramming, we generated multiple constructs expressing CD38 mutants (Figure 3B). T cells were nucleofected as previously described, subsequently transduced to introduce various CD38 mutant variants, and expanded according to standard procedures (Figure S4C). The expression of mutants was validated via flow cytometry (Figure S4D), and enzymatic activity was verified through high-performance liquid chromatography (HPLC) analysis. CD38 exhibits cyclase activity, enabling the conversion of NAD to cADPR, and hydrolase activity, converting cADPR to ADPR, which can be further metabolized to generate adenosine in the presence of CD203a and CD73 (Figure 3A). T cells were additionally activated with CD3/CD28 beads and stained to determine that T cells express CD73

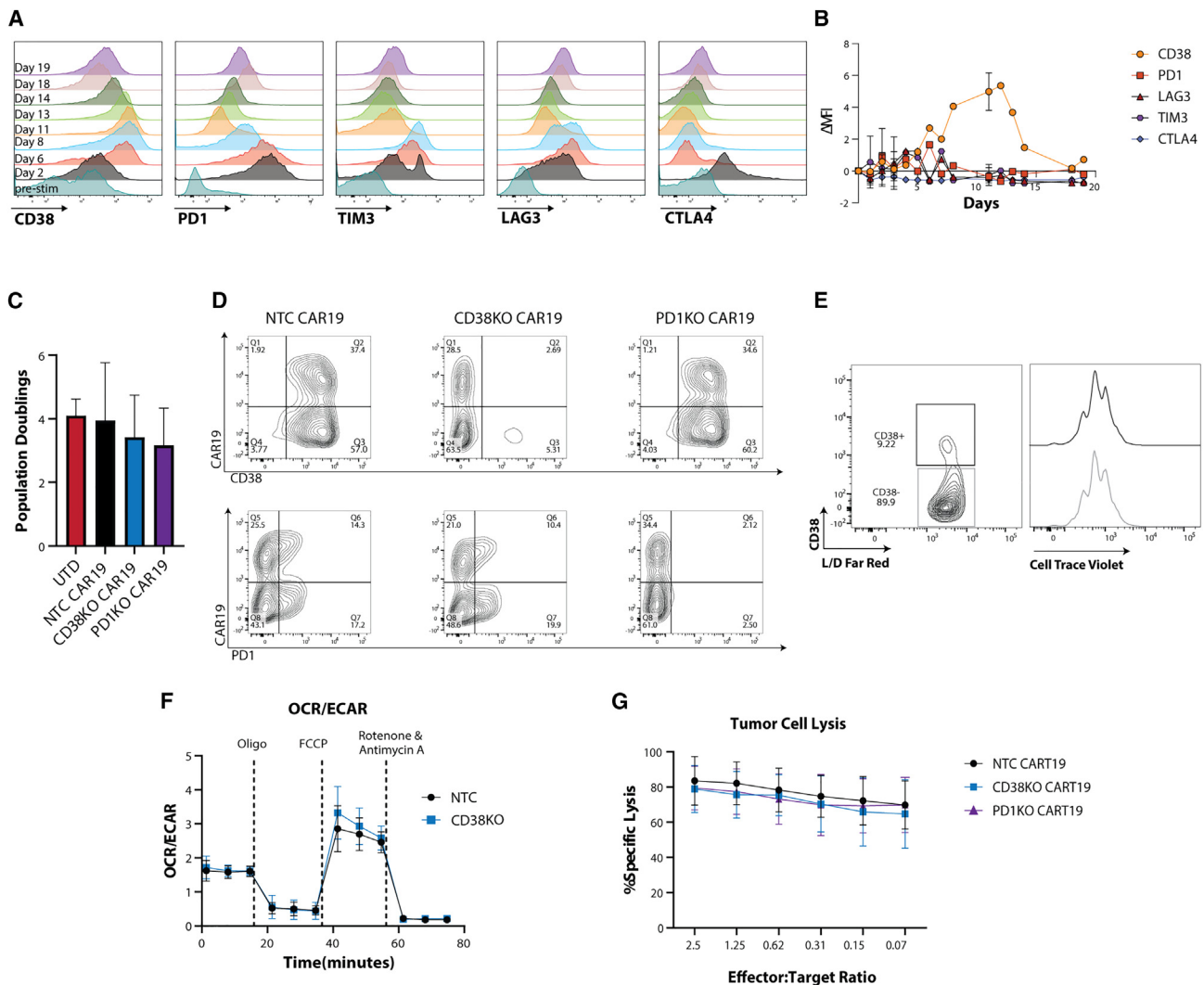


**Figure 1. Characterizing the effect of CD38KO on T cells in short-term *in vitro* assays**

(A) Normal human peripheral blood mononuclear cells (PBMCs;  $n = 3$ ) were stimulated with anti-CD3/CD28 beads on day 0. Flow cytometry was used to determine expression over time of CD38, PD1, TIM3, LAG3, and CTLA4 at the indicated time points. (B) Graph showing  $\Delta$ MFI (mean fluorescence intensity – baseline mean fluorescence intensity) over time. (C) CAR T cells were expanded based on standard protocol, where population doublings =  $\ln(\text{T cell count harvested}/\text{T cell count initial})/\ln(2)$  ( $n = 8$ ).<sup>34</sup> (D) Representative flow plots of surface expression of PD1, CD38, and CAR on non-transduced (NTC), CD38KO, and PD1KO CAR19 T cells. (E) Within CD38 KO CAR T cells, CD38+ and CD38– proliferation was measured by flow cytometry. (F) Seahorse assay was performed on day 7 of T cell expansion to determine OCR/ECAR metabolism ( $n = 3$ ) (74% average CD38KO). (G) CAR T cells were incubated at various effector-to-target (E:T) ratios with GFP/Luc+ Nalm6 cells for 24 h, and the remaining Luc+ Nalm6 was quantified to determine the percentage of specific lysis ( $(\text{experimental lysis} - \text{spontaneous lysis})/(\text{max lysis} - \text{spontaneous lysis}) * 100$ ) ( $n = 3$ ).

but not CD203a (Figure S4A). In CD38KO T cells, we observed the highest NAD concentration, the lowest cADPR concentration, and low levels of adenosine. Conversely, CD38WT (KO transduced to express wild-type CD38) exhibited the lowest NAD concentration and the highest adenosine levels. The CD38-decreased mutant, characterized by reduced hydrolase and cyclase activity, maintained high NAD levels, low adenosine levels, and intermediate cADPR levels, while the CD38-cyclase mutant, which can solely generate cADPR (excluding ADPR), exhibited the highest cADPR concentration, low NAD concentration, and intermediate to high adenosine

levels (Figure 3D). These findings confirm the enzymatic function of our constructs while also highlighting the significant impact of CD38's cyclase activity in utilizing NAD and ultimately producing adenosine, compared to its hydrolase activity. Performing principal-component analysis demonstrated distinctive groupings, where the CD38-decreased mutant exhibited a stronger correlation with CD38KO than with the CD38-cyclase mutant (Figure 3C). Initially, we expected that the CD38-decreased and CD38-cyclase mutants would exhibit distinct metabolic profiles, separate from CD38WT. However, the CD38-cyclase mutant displayed a

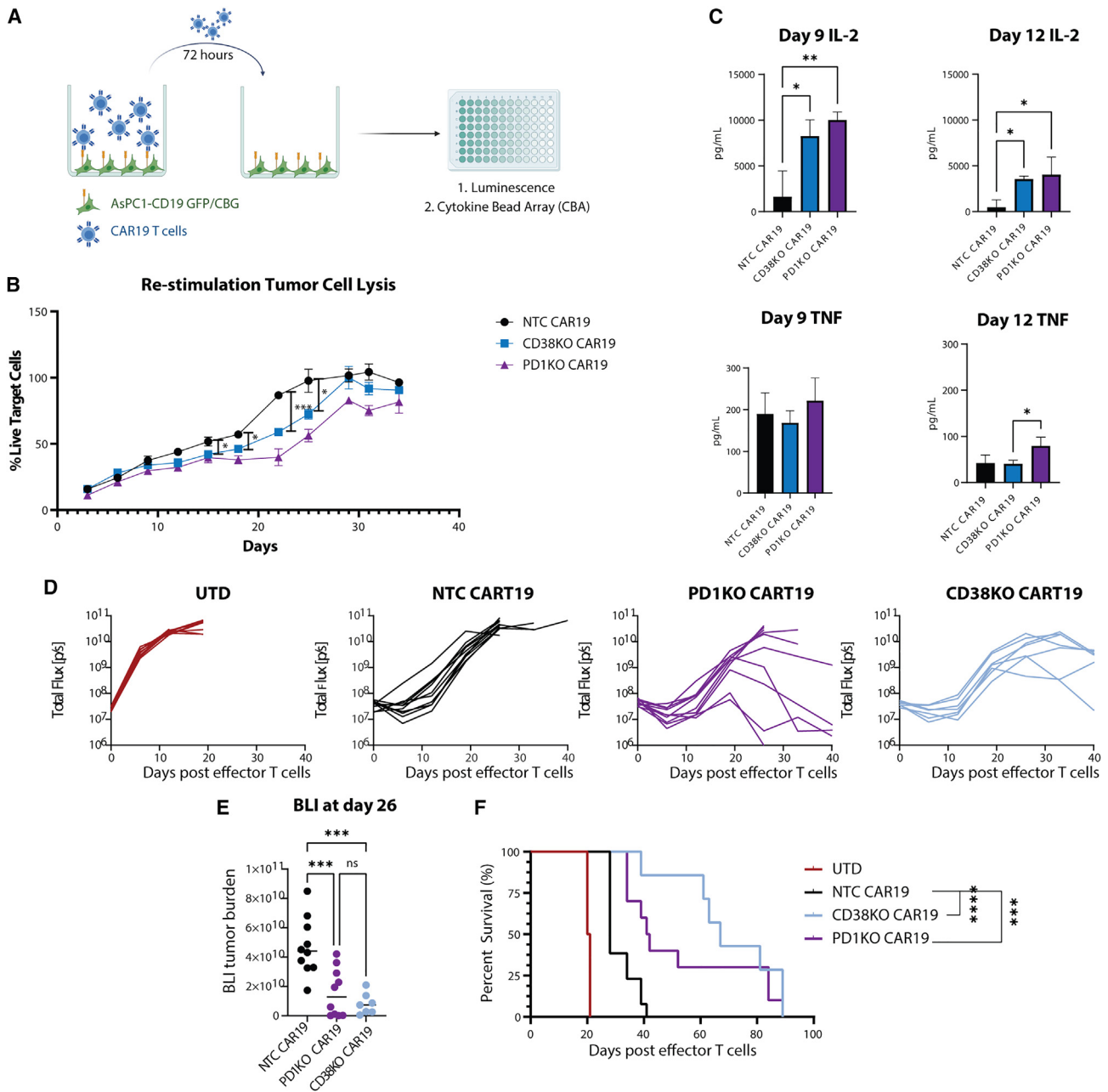


**Figure 2. CD38KO confers better long-term tumor control *in vitro* and longer mice survival *in vivo***

(A) Schematic representation of repeated long-term target stimulation *in vitro*, where GFP/Luc+ AsPC1-CD19 cells were incubated with CAR19 T cells at an E:T ratio of 1:0.15. Every 3 days, the remaining target cells were quantified by luminescence. Supernatant containing T cells was then added to a new plate containing freshly plated target cells. (B) Killing assay quantifying remaining percentage of target cells over time (representative of 4 donors). Error bars indicate mean with SD, comparison using two-way ANOVA with multiple comparisons. (C) Day 9 and 12 measurements of IL-2 and tumor necrosis factor (TNF). Error bars indicate mean with SD, comparison using one-way ANOVA with multiple comparisons.  $**p < 0.01$  and  $***p < 0.001$ . (D) Total flux images of mice over time separated by treatment group. (E) Kinetics on day 26 of tumor flux by luminescence of Nalm6 in NSG mice treated with UTD, NTC, CD38KO, and PD1KO CAR19 T cells. Error bars indicate mean with SD ( $n = 10$  mice). (F) Kaplan-Meier survival curves for mice treated with UTD, NTC, CD38KO, and PD1KO CAR19 T cells. Log-rank (Mantel-Cox) test performed.  $***p < 0.001$  and  $****p < 0.0001$  ( $n = 10$  mice).

metabolic signature resembling that of CD38KO, as seen when examining a heatmap of the top 25 metabolites in all groups (Figure 3E). To gain insight into metabolic pathways implicated in these

variations, we conducted a KEGG pathway enrichment analysis comparing CD38KO and CD38WT. This analysis revealed higher enrichment in pathways associated with arginine biosynthesis, as

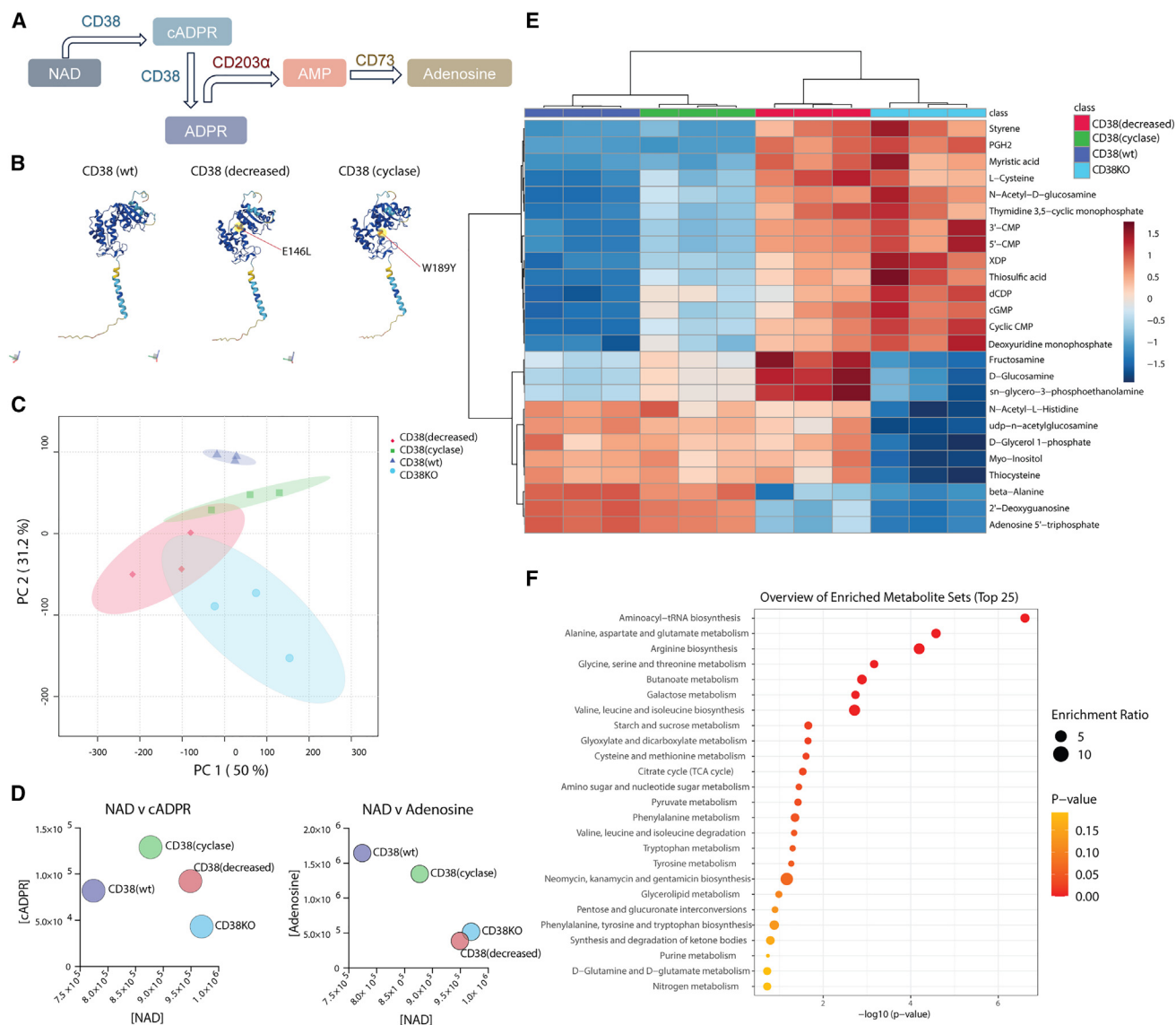


**Figure 3. Metabolic profiling of CD38KO and mutant expression in T cells**

(A) CD38 enzymatic pathway toward generation of adenosine. (B) Schematic representations of mutations on CD38 enzymatic pocket. (C) Principal-component analysis (PCA) of metabolites from T cells expressing either CD38KO, CD38WT, CD38 mutant with decreased enzymatic activity, and mutant with cyclase activity only. (D) Concentration comparison of NAD, cADPR, and adenosine expression in various CD38 CD38KO- or CD38mutant-expressing T cells. (E) Heatmap of top 25 differentially expressed metabolites between CD38KO, CD38(decreased), CD38(cyclase), and CD38KO T cells. (F) Metabolic pathway enrichment analysis between CD38KO and CD38(WT) T cells.

well as valine, leucine, and isoleucine metabolism in CD38-expressing cells (Figure 3F). These results provide insight for directing future research toward the most relevant metabolic pathways. Preliminary findings using carbon-labeled leucine (<sup>13</sup>CLeucine) suggested a decline in the percentage of acetyl-coenzyme A (CoA) and succinyl-CoA in CD38KO T cells (Figure S4B). This suggests that in CD38KO T cells, leucine is not utilized for energy production via the TCA cycle and may instead be directed toward an alternative pathway, such as mTOR signaling.<sup>35</sup> Further studies should

focus on elucidating specific mechanisms through which CD38 influences T cell metabolism.

## DISCUSSION

Despite exciting results from CAR T cell treatment of patients with hematologic malignancies, there is clearly still room for improvement.<sup>36</sup> It is likely that cell-intrinsic and cell-extrinsic mechanisms are responsible for CAR failures. T cell exhaustion ranks highly among cell-intrinsic mechanisms for CAR T failures, as it does in

other forms of T cell-based immunotherapy.<sup>36</sup> There is a wealth of potential molecular targets yet to be clinically validated, and preclinical data do not clearly identify a single most important node, molecule, or pathway. These observations suggest that there is scope for additional investigation into new or previously underappreciated inhibitory pathways in CAR T cells. In this work, we focused on CD38, a multifunctional ectoenzyme with significant NAD-hydrolyzing and adenosine-producing activities.<sup>18–20</sup> CD38 is recognized as a T cell activation marker, and as we have shown here, upon T cell stimulation, CD38 exhibits broadly similar kinetics to those of other, more widely accepted immune checkpoints. The potential for CD38 to play a counter-regulatory role in T cells is supported by its presence in dysfunctional and exhausted tumor-specific murine and human CD8 T cells.<sup>22,23</sup>

The role of CD38 in human CAR T cells specifically is less well defined. In 12 patients with B cell non-Hodgkin lymphoma (NHL) who were refractory to or relapsed after CART19 and received pembrolizumab to block the PD1/PD-L1 axis, CD38 expression clustered with other T cell exhaustion markers including PD1, CD39, TIGIT, TOX, and EOMES in immunophenotypically defined CAR-expressing T cells.<sup>10</sup> Furthermore, clusters enriched in patients who did not respond to PD1 inhibition were largely CD4+ T cells expressing the canonical exhaustion markers, including CD38. An independent dataset of peripheral blood 7 days post-CART19 found two CAR T cell meta clusters associated with progressive disease, of which one comprised CAR+ Tregs and the other was CD8+ T cells expressing typical exhaustion markers including CD39, CD101, CD244, TIGIT, and CD38.<sup>27</sup> Similarly, exhausted, tonically signaling GD2-specific CAR T cells costimulated with CD28 showed significant upregulation of CD38 along with other typical exhaustion genes when compared with functional non-tonically signaling GD2-specific CAR T cells costimulated with 41BB.<sup>37</sup> Finally, in a recently described *in vitro* chronic antigen exposure model, CD38 was among the upregulated genes in the highly exhausted NK-like CD8+ CAR T cell signature.<sup>38</sup>

While the deletion of CD38 in CAR NK cells has been described and may enhance their function,<sup>27,29</sup> here, we sought to investigate the effect of CD38 deletion in human CAR T cells. We hypothesized that CD38KO CAR T cells would exhibit some resistance to exhaustion, akin to that found by deleting PD1. We found that deletion of CD38 did not alter the basic properties of CAR T cells, such as proliferation after primary stimulation. Similarly, short-term functional assays such as cytotoxicity or cytokine production were not CD38 dependent, and in contrast to some of the published murine metabolic data,<sup>21</sup> we did not find differences in measures of oxidative phosphorylation or glycolysis. A potential role for CD38 emerged from experiments conducted on CAR T cells subjected to repeated *in vitro* stimulation, where superior tumor control was observed under CD38KO and PD1KO conditions. Further investigation revealed that exposure to a high tumor burden *in vivo* led to delayed tumor growth and prolonged survival. These findings suggested that internal cellular changes related to T cell metabolism, rather than

increased T cell proliferation or cytotoxicity, contributed to the observed effects. Our metabolomic data showed that CD38-deficient T cells produced lower amounts of adenosine and higher amounts of NAD+, leading us to speculate that upregulation of CD38 with T cell activation may provide a counter-regulatory role by producing the immunosuppressive metabolite adenosine and by depleting NAD+, an important oxidation-reduction substrate. The ability of CD38 to modulate the levels of NAD+, cADPR, and adenosine can profoundly affect the metabolic status of T cells, thereby exerting a significant influence on their function and responsiveness to immune responses.

The distinct pathway through which CD38 induces exhaustion or dysfunction in T cells, when combined with other inhibitory receptors, holds promise for enhanced therapy. Our research contributes to the potential application of combination therapy involving CD38KO and PD1KO CAR T cells. While not directly evaluated in our study, previous research has explored various forms of anti-CD38 and anti-PD1 combination therapy. For instance, a study involving patients with non-small cell lung cancer and metastatic prostate cancer treated with isatuximab (anti-CD38 antibody) and cemiplimab (anti-PD1 antibody) did not yield significant differences in overall outcome and survival.<sup>39</sup> In another study involving patients with multiple myeloma, the combination therapy of daratumumab (anti-CD38) and nivolumab (anti-PD1) was found to be more effective in controlling tumor burden compared to either therapy alone.<sup>40</sup> Additionally, a study using an anti-CD38 enzymatic inhibitor (Rhein) in conjunction with anti-PD1 therapy showed enhanced tumor control in a mouse model of lung cancer.<sup>24</sup> Therefore, targeting not only CD38 but specifically its enzymatic activity in combination with PD1KO could offer significant benefits, as they employ distinct mechanisms of resistance, potentially resulting in stronger resistance against T cell exhaustion. While further experiments are required to precisely define the mechanisms by which CD38 functions as an immunometabolism checkpoint molecule, this research suggests that CD38 could be a valuable addition to the repertoire of genetic modifications aimed at enhancing CAR T cell function.

## MATERIALS AND METHODS

### Single-cell RNA sequencing analysis

The processed data were downloaded from NCBI GEO (GEO: GSE139324),<sup>41</sup> subsetted down to 20,000 cells, and processed through the standard workflow from Seurat v.4 without additional filtering. Cell-type identities were assigned using single-cell reference mapping using an annotated PBMC reference dataset.<sup>42</sup>

### Cell lines and culture

The Nalm6 cell line was obtained from American Type Culture Collection and cultured in RPMI 1640 with 10% FBS, 1% penicillin/streptomycin, 1% HEPES, and 1% GlutaMAX and kept at 37°C in 5% CO<sub>2</sub>. Nalm6 click beetle green (CBG) and GFP were generated by lentiviral transduction and sorted for >99% purity. The AspC1-CD19 (CBG/GFP) cell line was a gift from the lab of Dr. Carl June.

### CRISPR-Cas9 genomic engineering

Guide RNAs for targeting CD38 (5'-AGTGTATGGGATGCTTTCAA-3') and PD1 (5'-GGCCAGGATGGTTCTTAGGT-3') were a gift from the lab of Dr. Carl June and were chemically synthesized by Integrated DNA Technologies (IDT). Gene deletion was done by electroporating T cells using the Lonza 4D Nucleofector Core/X Unit and the P3 Primary Cell 4D Kit (Lonza). The CRISPR ribonucleoprotein (RNP) complex was formed by incubating 10 µg of Sp HiFi Cas9 (IDT) with 5 µg of sgRNA (IDT) for 10 min at room temperature. Cells were spun at  $300 \times g$  for 10 min and then resuspended at a concentration of  $5\text{--}10 \times 10^6$  cells/100 µL Primary P3 buffer. 100 µL of cells and RNP complex were transferred into a cuvette, and the pulse code EH115 was used. Cells were immediately quenched in 1 mL of media and kept at  $5 \times 10^6$  cells/mL at 30°C for 24 h with 5 ng/mL of IL-7 and IL-15.

### T cell manufacturing

The pTRPE anti-CD19-41BB-CD3ζ (CAR19) and pTRPE anti-CD123-41BB-CD3ζ (CAR123) plasmid DNAs were generated as previously reported.<sup>33,43</sup> Normal donor healthy human T cells were obtained from the University of Pennsylvania Human Immunology Core. These cells were modified using CRISPR-Cas9 RNP and kept at 30°C for 24 h with 5 ng/mL IL-7 and IL-15 (Peprotech). Cells were then activated using Dynabeads CD3/CD28 (Thermo Scientific) at a 3:1 bead-to-cell ratio and maintained in X-Vivo15 with 5% human serum, 1% penicillin/streptomycin, 1% HEPES, and 1% GlutaMAX. Transduction of anti-CD19 CAR lentivirus or anti-CD123 CAR lentivirus was done 24 h after bead stimulation at an MOI of 3. Dynabeads were removed on day 6–7 of stimulation, and cells were counted and maintained at  $8 \times 10^5$  cells/mL using the Multisizer Coulter Counter (Beckman Coulter) until the mean cell volume was below 350 fL.

### Flow cytometry

Antibodies were purchased from BioLegend, Invitrogen, or eBioscience. CD19 CAR was detected by an anti-CD19 scFv derived from FMC69 conjugated to PE. Cells were stained with fluorophore-conjugated antibodies at 4°C for 30 min. Cell viability was measured using either Live/Dead Aqua or Live/Dead Violet fixable staining kit (Life Technologies) according to the manufacturer's instructions. Proliferation was performed using the CellTrace Violet Proliferation Kit (Thermo Scientific) according to the manufacturer's instructions. Samples were acquired on an LSRII Fortessa Cytometer (BS Biosciences). All data analysis was performed using FlowJo10.0 software (FlowJo). Populations of interest were identified by gating forward versus side scatter, singlet gating, and the exclusion of dead cells using Live/Dead dyes. Surface expression of CD38 mutants was detected by incubating cells with anti-myc tag antibody conjugated to a fluorophore.

### Bioluminescence-based cytotoxic killing assays

The Nalm6 (GFP/CBG) cell line was used in killing assays, and cell survival was measured by quantification of bioluminescence. For short-term killing assays (24 h), target Nalm6 GFP/CBG cells were

seeded at  $1 \times 10^5$  cells/mL, and effector CAR T cells were added at various effector-to-target ratios. Cells were incubated at 37°C in 5% CO<sub>2</sub> for 24 h, and then bioluminescence was detected and quantified using the Bio Tek Synergy H4 imager and Gen5 software. Triplicates were averaged, and data were calculated using the formula: % specific lysis =  $100 \times (\text{tumor only} - \text{test sample lysis}) / (\text{tumor only} - \text{max lysis})$ , where max lysis = 0. For restimulation killing assays.

### Mouse model experiments

The University of Pennsylvania Animal Care and Use Committee approved all animal experiments, and all procedures were performed in the animal facility at the University of Pennsylvania in accordance with the Federal and Institutional Animal Care and Use Committee requirements. Male and female 6- to 8-week-old NSG mice were purchased from the Jackson Laboratory or bred in house and maintained in pathogen-free conditions. Animals were injected via tail vein with  $5 \times 10^5$  Nalm6 (GFP/CBG) cells in 200 µL sterile PBS. Seven days after tumor injection, mice were randomized on the basis of tumor burden, and  $1\text{--}2 \times 10^6$  T cells (CAR+) were injected via tail vein in 200 µL of sterile PBS. Tumor burden was measured weekly by bioluminescent imaging. Imaging data were analyzed using LivingImage v.4.4 (Caliper LifeSciences, PerkinElmer). Peripheral blood was obtained via retro-orbital bleeding biweekly, and cell numbers were quantified using CountBright Absolute Counting Beads (Thermo Scientific) using flow cytometry. Animals were observed for body weight loss exceeding 20%, fur loss, and hindlimb paralysis.

### Metabolic assays

The T cell OCR and ECAR were measured using the Seahorse XF69 Extracellular Flux Analyzer following established protocols. In brief, activated T cells ( $1.5 \times 10^5$ ) were plated on Cell-Tak-coated XF96 plates via centrifugation in XF RPMI medium. Cellular bioenergetics were assessed by sequential addition of oligomycin, fluorocarbonyl cyanide phenylhydrazone, and rotenone/antimycin A. In brief, T cells for ultra-performance liquid chromatography (UPLC)-mass spectrometry (MS) were counted ( $2\text{--}5 \times 10^6$ ), washed with PBS, and spun down  $300 \times g$  for 5 min. Cells were then resuspended with a  $-80^\circ\text{C}$  mixture of ACN/methanol/water and pulse sonicated before being spun down again. Supernatant was then allowed to dry under nitrogen and resuspended with 5% 5-sulfosalicylic acid (SSA). Samples were then sonicated and spun down, and finally, supernatant was transferred into HPLC vials and stored at 4°C until further processing. All metabolites were measured based on untargeted and targeted UPLC-MS, and metabolite intensities were normalized. Agilent MassHunter Software was used for raw data acquisition and processing. MetaboAnalyst and GraphPad Prism were used for data visualization.

### Statistical analysis

All statistical analysis was performed using GraphPad Prism, where comparisons between groups were performed using either unpaired t test or ordinary one-way ANOVA with Turkey's multiple comparison test. Unless noted otherwise, data are reported as mean  $\pm$  SD. Survival data were analyzed using the log-rank (Mantel-Cox) test.

## DATA AND CODE AVAILABILITY

All data associated with this study are present in the manuscript. Materials used in this study are available from the corresponding author upon reasonable request.

## SUPPLEMENTAL INFORMATION

Supplemental information can be found online at <https://doi.org/10.1016/j.omton.2024.200819>.

## ACKNOWLEDGMENTS

This study was supported by the Hematology Clinical Research NIH T32 HL0439 grant and by a Specialized Center of Research (SCOR) grant from the Leukemia & Lymphoma Society “Pan-Heme CAR anti-CD38 CAR T cells for myeloid, lymphoid and plasma cell malignancies.”

## AUTHOR CONTRIBUTIONS

Conceptualization, K.V. and S.G.; funding acquisition, S.G.; writing – original draft, K.V.; writing – review & editing, K.V. and S.G.; data curation, K.V., F.S., A.S., M.S., O.S., R.S.O., S.S., and T.H.; data visualization, K.V., R.S.O., S.G., M.S., A.S., S.S., and T.H.; formal analysis, K.V., R.S.O., and S.G.

## DECLARATION OF INTERESTS

S.G. has patents related to CAR therapy with royalties paid from Novartis to the University of Pennsylvania. S.G. is a scientific cofounder and holds equity in Interius Biotherapeutics and Carisma Therapeutics. S.G. is a scientific advisor to Carisma, Cartography, Currus, Interius, Kite, NKILT, Mission Bio, and Vor Bio.

## REFERENCES

- Blank, C.U., Haining, W.N., Held, W., Hogan, P.G., Kallies, A., Lugli, E., Lynn, R.C., Philip, M., Rao, A., Restifo, N.P., et al. (2019). Defining T cell exhaustion. *Nat. Rev. Immunol.* 19, 665–674. <https://doi.org/10.1038/s41577-019-0221-9>.
- Collier, J.L., Weiss, S.A., Pauken, K.E., Sen, D.R., and Sharpe, A.H. (2021). Not-so-opposite ends of the spectrum: CD8+ T cell dysfunction across chronic infection, cancer and autoimmunity. *Nat. Immunol.* 22, 809–819. <https://doi.org/10.1038/s41590-021-00949-7>.
- Morad, G., Helmink, B.A., Sharma, P., and Wargo, J.A. (2021). Hallmarks of response, resistance, and toxicity to immune checkpoint blockade. *Cell* 184, 5309–5337. <https://doi.org/10.1016/j.cell.2021.09.020>.
- Cherkassky, L., Morello, A., Villena-Vargas, J., Feng, Y., Dimitrov, D.S., Jones, D.R., Sadelain, M., and Adusumilli, P.S. (2016). Human CAR T cells with cell-intrinsic PD-1 checkpoint blockade resist tumor-mediated inhibition. *J. Clin. Invest.* 126, 3130–3144. <https://doi.org/10.1172/JCI83092>.
- Rafiq, S., Yeku, O.O., Jackson, H.J., Purdon, T.J., Van Leeuwen, D.G., Drakes, D.J., Song, M., Miele, M.M., Li, Z., Wang, P., et al. (2018). Targeted delivery of a PD-1 blocking scFv by CAR-T cells enhances anti-tumor efficacy in vivo. *Nat. Biotechnol.* 36, 847–856. <https://doi.org/10.1038/nbt.4195>.
- Agarwal, S., Aznar, M.A., Rech, A.J., Good, C.R., Kuramitsu, S., Da, T., Gohil, M., Chen, L., Hong, S.-J.A., Ravikumar, P., et al. (2023). Deletion of the inhibitory co-receptor CTLA-4 enhances and invigorates chimeric antigen receptor T cells. *Immunity* 56, 2388–2407.e9. <https://doi.org/10.1016/j.immuni.2023.09.001>.
- Heczey, A., Louis, C.U., Savoldo, B., Dakhova, O., Durett, A., Grilley, B., Liu, H., Wu, M.F., Mei, Z., Gee, A., et al. (2017). CAR T Cells Administered in Combination with Lymphodepletion and PD-1 Inhibition to Patients with Neuroblastoma. *Mol. Ther.* 25, 2214–2224. <https://doi.org/10.1016/j.yimthe.2017.05.012>.
- Grosser, R., Cherkassky, L., Chintala, N., and Adusumilli, P.S. (2019). Combination Immunotherapy with CAR T Cells and Checkpoint Blockade for the Treatment of Solid Tumors. *Cancer Cell* 36, 471–482. <https://doi.org/10.1016/j.ccell.2019.09.006>.
- Stadtmauer, E.A., Fraietta, J.A., Davis, M.M., Cohen, A.D., Weber, K.L., Lancaster, E., Mangan, P.A., Kulikovskaya, I., Gupta, M., Chen, F., et al. (2020). CRISPR-engineered T cells in patients with refractory cancer. *Science* 367, eaba7365. <https://doi.org/10.1126/science.aba7365>.
- Chong, E.A., Alanio, C., Svoboda, J., Nasta, S.D., Landsburg, D.J., Lacey, S.F., Ruella, M., Bhattacharyya, S., Wherry, E.J., and Schuster, S.J. (2022). Pembrolizumab for B-cell lymphomas relapsing after or refractory to CD19-directed CAR T-cell therapy. *Blood* 139, 1026–1038. <https://doi.org/10.1182/blood.2021012634>.
- Wolf, Y., Anderson, A.C., and Kuchroo, V.K. (2020). TIM3 comes of age as an inhibitory receptor. *Nat. Rev. Immunol.* 20, 173–185. <https://doi.org/10.1038/s41577-019-0224-6>.
- Patsoukis, N., Wang, Q., Strauss, L., and Boussiotis, V.A. (2020). Revisiting the PD-1 pathway. *Sci. Adv.* 6, eabd2712. <https://doi.org/10.1126/sciadv.abd2712>.
- Graydon, C.G., Mohideen, S., and Fowke, K.R. (2020). LAG3's Enigmatic Mechanism of Action. *Front. Immunol.* 11, 615317. <https://doi.org/10.3389/fimmu.2020.615317>.
- Walker, L.S.K., and Sansom, D.M. (2011). The emerging role of CTLA4 as a cell-extrinsic regulator of T cell responses. *Nat. Rev. Immunol.* 11, 852–863. <https://doi.org/10.1038/nri3108>.
- Simoni, Y., Becht, E., Fehlings, M., Loh, C.Y., Koo, S.-L., Teng, K.W.W., Yeong, J.P.S., Nahar, R., Zhang, T., Kared, H., et al. (2018). Bystander CD8+ T cells are abundant and phenotypically distinct in human tumour infiltrates. *Nature* 557, 575–579. <https://doi.org/10.1038/s41586-018-0130-2>.
- Allard, D., Allard, B., and Stagg, J. (2020). On the mechanism of anti-CD39 immune checkpoint therapy. *J. Immunother. Cancer* 8, e000186. <https://doi.org/10.1136/jitc-2019-000186>.
- Mitra, A., Thompson, B., Strange, A., Amato, C.M., Vassallo, M., Dolgalev, I., Hester-McCullough, J., Muramatsu, T., Kimono, D., Puranik, A.S., et al. (2023). A Population of Tumor-Infiltrating CD4+ T Cells Co-Expressing CD38 and CD39 Is Associated with Checkpoint Inhibitor Resistance. *Clin. Cancer Res.* 29, 4242–4255. <https://doi.org/10.1158/1078-0432.CCR-23-0653>.
- Hogan, K.A., Chini, C.C.S., and Chini, E.N. (2019). The Multi-faceted Ecto-enzyme CD38: Roles in Immunomodulation, Cancer, Aging, and Metabolic Diseases. *Front. Immunol.* 10, 1187. <https://doi.org/10.3389/fimmu.2019.01187>.
- Chini, C.C.S., Peclat, T.R., Warner, G.M., Kashyap, S., Espindola-Netto, J.M., De Oliveira, G.C., Gomez, L.S., Hogan, K.A., Tarragó, M.G., Puranik, A.S., et al. (2020). CD38 ecto-enzyme in immune cells is induced during aging and regulates NAD+ and NMN levels. *Nat. Metab.* 2, 1284–1304. <https://doi.org/10.1038/s42255-020-00298-z>.
- Aksoy, P., White, T.A., Thompson, M., and Chini, E.N. (2006). Regulation of intracellular levels of NAD: A novel role for CD38. *Biochem. Biophys. Res. Commun.* 345, 1386–1392. <https://doi.org/10.1016/j.bbrc.2006.05.042>.
- Chatterjee, S., Daenthanasamak, A., Chakraborty, P., Wyatt, M.W., Dhar, P., Selvam, S.P., Fu, J., Zhang, J., Nguyen, H., Kang, I., et al. (2018). CD38-NAD+ Axis Regulates Immunotherapeutic Anti-Tumor T Cell Response. *Cell Metab.* 27, 85–100.e8. <https://doi.org/10.1016/j.cmet.2017.10.006>.
- Philip, M., Fairchild, L., Sun, L., Horste, E.L., Camara, S., Shakiba, M., Scott, A.C., Viale, A., Lauer, P., Merghoub, T., et al. (2017). Chromatin states define tumour-specific T cell dysfunction and reprogramming. *Nature* 545, 452–456. <https://doi.org/10.1038/nature22367>.
- Verma, V., Shrimali, R.K., Ahmad, S., Dai, W., Wang, H., Lu, S., Nandre, R., Gaur, P., Lopez, J., Sade-Feldman, M., et al. (2019). PD-1 blockade in subprimed CD8 cells induces dysfunctional PD-1+CD38hi cells and anti-PD-1 resistance. *Nat. Immunol.* 20, 1231–1243. <https://doi.org/10.1038/s41590-019-0441-y>.
- Chen, L., Diao, L., Yang, Y., Yi, X., Rodriguez, B.L., Li, Y., Villalobos, P.A., Cascone, T., Liu, X., Tan, L., et al. (2018). CD38-Mediated Immunosuppression as a Mechanism of Tumor Cell Escape from PD-1/PD-L1 Blockade. *Cancer Discov.* 8, 1156–1175. <https://doi.org/10.1158/2159-8290.CD-17-1033>.
- Kar, A., Ghosh, P., Gautam, A., Chowdhury, S., Basak, D., Sarkar, I., Bhoumik, A., Barman, S., Chakraborty, P., Mukhopadhyay, A., et al. (2024). CD38–RyR2 axis-mediated signaling impedes CD8 + T cell response to anti-PD1 therapy in cancer.



- Proc. Natl. Acad. Sci. USA 121, e2315989121. <https://doi.org/10.1073/pnas.2315989121>.
26. Li, C., Phoon, Y.P., Karlinsey, K., Tian, Y.F., Thapaliya, S., Thongkum, A., Qu, L., Matz, A.J., Cameron, M., Cameron, C., et al. (2022). A high OXPHOS CD8 T cell subset is predictive of immunotherapy resistance in melanoma patients. *J. Exp. Med.* 219, e20202084. <https://doi.org/10.1084/jem.20202084>.
  27. Naeimi Kararoudi, M., Nagai, Y., Elmas, E., De Souza Fernandes Pereira, M., Ali, S.A., Imus, P.H., Wethington, D., Borrello, I.M., Lee, D.A., and Ghiaur, G. (2020). CD38 deletion of human primary NK cells eliminates daratumumab-induced fratricide and boosts their effector activity. *Blood* 136, 2416–2427. <https://doi.org/10.1182/blood.202006200>.
  28. Woan, K.V., Kim, H., Bjordahl, R., Davis, Z.B., Gaidarova, S., Goulding, J., Hancock, B., Mahmood, S., Abujarour, R., Wang, H., et al. (2021). Harnessing features of adaptive NK cells to generate iPSC-derived NK cells for enhanced immunotherapy. *Cell Stem Cell* 28, 2062–2075.e5. <https://doi.org/10.1016/j.stem.2021.08.013>.
  29. Clara, J.A., Levy, E.R., Reger, R., Barisic, S., Chen, L., Cherkasova, E., Chakraborty, M., Allan, D.S.J., and Childs, R. (2022). High-affinity CD16 integration into a CRISPR/Cas9-edited CD38 locus augments CD38-directed antitumor activity of primary human natural killer cells. *J. Immunother. Cancer* 10, e003804. <https://doi.org/10.1136/jitc-2021-003804>.
  30. Liao, C., Wang, Y., Huang, Y., Duan, Y., Liang, Y., Chen, J., Jiang, J., Shang, K., Zhou, C., Gu, Y., et al. (2023). CD38-Specific CAR Integrated into CD38 Locus Driven by Different Promoters Causes Distinct Antitumor Activities of T and NK Cells. *Adv. Sci.* 10, 2207394. <https://doi.org/10.1002/advs.202207394>.
  31. Huang, Y., Shao, M., Teng, X., Si, X., Wu, L., Jiang, P., Liu, L., Cai, B., Wang, X., Han, Y., et al. (2024). Inhibition of CD38 enzymatic activity enhances CAR-T cell immunotherapeutic efficacy by repressing glycolytic metabolism. *Cell Rep. Med.* 5, 101400. <https://doi.org/10.1016/j.xcrm.2024.101400>.
  32. Good, Z., Spiegel, J.Y., Sahaf, B., Malipatlolla, M.B., Ehlinger, Z.J., Kurra, S., Desai, M.H., Reynolds, W.D., Wong Lin, A., Vandris, P., et al. (2022). Post-infusion CAR TReg cells identify patients resistant to CD19-CAR therapy. *Nat. Med.* 28, 1860–1871. <https://doi.org/10.1038/s41591-022-01960-7>.
  33. Milone, M.C., Fish, J.D., Carpenito, C., Carroll, R.G., Binder, G.K., Teachey, D., Samanta, M., Lakhai, M., Gloss, B., Danet-Desnoyers, G., et al. (2009). Chimeric Receptors Containing CD137 Signal Transduction Domains Mediate Enhanced Survival of T Cells and Increased Antileukemic Efficacy In Vivo. *Mol. Ther.* 17, 1453–1464. <https://doi.org/10.1038/mt.2009.83>.
  34. Coeshott, C., Vang, B., Jones, M., and Nankervis, B. (2019). Large-scale expansion and characterization of CD3+ T-cells in the Quantum® Cell Expansion System. *J. Transl. Med.* 17, 258. <https://doi.org/10.1186/s12967-019-2001-5>.
  35. Ananieva, E.A., Powell, J.D., and Hutson, S.M. (2016). Leucine Metabolism in T Cell Activation: mTOR Signaling and Beyond. *Adv. Nutr.* 7, 798S–805S. <https://doi.org/10.3945/an.115.011221>.
  36. Labanieh, L., and Mackall, C.L. (2023). CAR immune cells: design principles, resistance and the next generation. *Nature* 614, 635–648. <https://doi.org/10.1038/s41586-023-05707-3>.
  37. Long, A.H., Haso, W.M., Shern, J.F., Wanhainen, K.M., Murgai, M., Ingaramo, M., Smith, J.P., Walker, A.J., Kohler, M.E., Venkateshwara, V.R., et al. (2015). 4-1BB costimulation ameliorates T cell exhaustion induced by tonic signaling of chimeric antigen receptors. *Nat. Med.* 21, 581–590. <https://doi.org/10.1038/nm.3838>.
  38. Good, C.R., Aznar, M.A., Kuramitsu, S., Samareh, P., Agarwal, S., Donahue, G., Ishiyama, K., Wellhausen, N., Rennels, A.K., Ma, Y., et al. (2021). An NK-like CAR T cell transition in CAR T cell dysfunction. *Cell* 184, 6081–6100.e26. <https://doi.org/10.1016/j.cell.2021.11.016>.
  39. Zucali, P.A., Lin, C.-C., Carthon, B.C., Bauer, T.M., Tucci, M., Italiano, A., Iacovelli, R., Su, W.-C., Massard, C., Saleh, M., et al. (2022). Targeting CD38 and PD-1 with isatuximab plus cemiplimab in patients with advanced solid malignancies: results from a phase I/II open-label, multicenter study. *J. Immunother. Cancer* 10, e003697. <https://doi.org/10.1136/jitc-2021-003697>.
  40. Verkleij, C.P.M., Jhatakia, A., Broekmans, M.E.C., Frerichs, K.A., Zweegman, S., Mutis, T., Bezman, N.A., and Van De Donk, N.W.C.J. (2020). Preclinical Rationale for Targeting the PD-1/PD-L1 Axis in Combination with a CD38 Antibody in Multiple Myeloma and Other CD38-Positive Malignancies. *Cancers* 12, 3713. <https://doi.org/10.3390/cancers12123713>.
  41. Cillo, A.R., Kürten, C.H.L., Tabib, T., Qi, Z., Onkar, S., Wang, T., Liu, A., Duvvuri, U., Kim, S., Soose, R.J., et al. (2020). Immune Landscape of Viral- and Carcinogen-Driven Head and Neck Cancer. *Immunity* 52, 183–199.e9. <https://doi.org/10.1016/j.immuni.2019.11.014>.
  42. Hao, Y., Hao, S., Andersen-Nissen, E., Mauck, W.M., Zheng, S., Butler, A., Lee, M.J., Wilk, A.J., Darby, C., Zager, M., et al. (2021). Integrated analysis of multimodal single-cell data. *Cell* 184, 3573–3587.e29. <https://doi.org/10.1016/j.cell.2021.04.048>.
  43. Gill, S., Tasian, S.K., Ruella, M., Shestova, O., Li, Y., Porter, D.L., Carroll, M., Danet-Desnoyers, G., Scholler, J., Grupp, S.A., et al. (2014). Preclinical targeting of human acute myeloid leukemia and myeloablation using chimeric antigen receptor–modified T cells. *Blood* 123, 2343–2354. <https://doi.org/10.1182/blood-2013-09-529537>.